

Gaussian distribution of inhomogeneous neutrino degeneracy and big bang nucleosynthesis

Spencer D. Stirling

*Department of Physics and Department of Mathematics
University of Utah, Salt Lake City, Utah 84112*

Robert J. Scherrer

*Department of Physics and Department of Astronomy
The Ohio State University, Columbus, Ohio 43210*

Research funded by the National Science Foundation Research Experience for Undergraduates (REU) at The Ohio State University, Summer 2000

We explore the effect of inhomogeneous neutrino degeneracy on big bang nucleosynthesis (BBN) in the case where such inhomogeneity is described by a Gaussian distribution. In particular, two cases are investigated: equal degeneracy for all three neutrino flavors, and electron-neutrino degeneracy alone. We show that element abundances increase with Gaussian width, and we conclude that Gaussian inhomogeneity actually narrows the range of the baryon-to-photon ratio η .

1 Introduction

Several modifications [1] to the standard model of big bang nucleosynthesis (BBN) [2, 3] have been explored in an effort to relax ever-tightening constraints produced by observational data. In particular, allowing for a neutrino degeneracy, i.e. an asymmetry between neutrinos and antineutrinos, is one variant with interesting consequences [4, 5]. Indeed, several others [6, 7, 8] have introduced fresh models which produce such a neutrino degeneracy.

Dolgov and Pagel [11] more recently proposed *inhomogeneous* neutrino degeneracy in response to observational variations in the deuterium abundance in high-redshift Lyman-alpha clouds. We follow suit and propose an inhomogeneous neutrino-degenerate universe in the form of a cluster of horizon volumes which may vary in neutrino degeneracy from one another, but within each are uniform. Thus, inside each horizon volume we can assume that BBN occurs as it does in the case of homogeneous neutrino degeneracy. We then assume a weight distribution which describes the overall fraction of horizon volumes that have a given neutrino degeneracy, and thus we can determine overall average element abundances. Here we have chosen a Gaussian distribution for our weight function, and we explore such element abundances (helium-4, deuterium, and lithium-7) for varying Gaussian means and widths. Effectively, we show that,

in most cases of interest, broad weight functions (more inhomogeneity) result in an increase in element abundances over the homogeneous cases alone.

But first we discuss briefly the standard model of BBN. In Sec. 3 we introduce the physical effects of homogeneous neutrino degeneracy, and in Sec. 4 we expand upon our technique for modeling an inhomogeneous universe. Finally, we analyze the results of our inhomogeneous model in Sec. 5.

2 Standard model

Assuming a standard Friedmann model [2, 3], at temperature $T \approx 200 \text{ MeV} \approx m_{\mu^-} + m_{\mu^+}$ the universe contains a thermal mixture of photons, neutrino-antineutrino pairs, electron-positron pairs, and muon-antimuon pairs. Furthermore, a small number of relic protons and neutrons remain from an earlier, hotter time because these baryons cannot be created at $T \leq 200 \text{ MeV}$.

As the temperature drops, i.e. $T \leq m_{\mu}$, the muon-antimuon pairs begin to annihilate. The overall muon/antimuon number density falls as $\exp(-m_{\mu}/kT)$ and essentially vanishes at $T \sim 10 \text{ MeV}$. This allows the neutrinos to thermally decouple from matter (and each other) since they remain in equilibrium through muon/antimuon reactions such as

$$\begin{aligned} e^- + \mu^+ &\leftrightarrow \nu_e + \bar{\nu}_\mu & e^+ + \mu^- &\leftrightarrow \bar{\nu}_e + \nu_\mu \\ \nu_e + \mu^- &\leftrightarrow \nu_\mu + e^- & \bar{\nu}_e + \mu^+ &\leftrightarrow \bar{\nu}_\mu + e^+ \\ \nu_\mu + \mu^+ &\leftrightarrow \nu_e + e^+ & \bar{\nu}_\mu - \mu^+ &\leftrightarrow \bar{\nu}_e + e^-. \end{aligned} \quad (1)$$

It may, however, be possible for electron-neutrinos to remain coupled down to $T \sim 2 - 3 \text{ MeV}$ through reactions such as

$$e^- + e^+ \leftrightarrow \nu_e + \bar{\nu}_e \quad e^\pm + \nu_e \leftrightarrow e^\pm + \nu_e \quad e^\pm + \bar{\nu}_e \leftrightarrow e^\pm + \bar{\nu}_e. \quad (2)$$

Hence, we define the photon temperature T and the neutrino temperature T_ν separately. Note that, as $T \leq m_e$ the electron-positron pairs annihilate into photons, the end result being a rise in photon temperature T relative to T_ν . In particular, for $T \ll m_e$ we have $T \approx 1.4 T_\nu$ [4].

Because the temperature plummets further, the relic baryon abundances begin to favor protons over neutrons. The overall neutron abundance at the onset of BBN will determine the final mass fraction of helium-4, and so we must calculate it as a function of temperature. Consider the following reactions

$$\nu_e + n \leftrightarrow p + e^- \quad e^+ + n \leftrightarrow p + \bar{\nu}_e \quad p + e^- + \bar{\nu}_e \rightarrow n \quad (3)$$

$$n \rightarrow p + e^- + \bar{\nu}_e. \quad (4)$$

As long as the corresponding reaction rates λ are high enough, the equilibrium ratio of the neutron number density n_n and the proton number density n_p should obey a Boltzmann distribution

$$\frac{n_n}{n_p} \approx \exp \left[\frac{-(m_n - m_p)}{T} \right]. \quad (5)$$

Defining the neutron fraction $X_n = \frac{n_n}{n_n + n_p}$ we quickly see

$$X_n(T) \approx \left[1 + \exp \left[\frac{m_n - m_p}{T} \right] \right]^{-1}. \quad (6)$$

At higher temperatures the neutron fraction approaches $\frac{1}{2}$, i.e. equal numbers of protons and neutrons, but at lower temperatures it diminishes as some neutrons decay into protons.

Eq. (6) suits our purpose only as long as the reaction rates λ are high enough. But at some temperature, say T_{freeze} , the two and three-body reactions (3) freeze out, leaving only neutron decay (4). Let $X_{n(freeze)}$ denote (6) evaluated at temperature T_{freeze} . Since neutron decay now dominates, we have

$$X_n(t) \approx X_{n(freeze)} \exp \left[-\frac{t}{1013 \text{ sec}} \right], \quad (7)$$

where $\lambda = (1013 \text{ sec})^{-1}$ is the reaction rate for neutron decay [4, pg 550]. From the Friedmann model in this temperature range [4, pg 538],

$$t \approx 0.8 \text{ sec} \left[\frac{1 \text{ MeV}}{T} \right]^2 \quad (8)$$

and so

$$X_n(T) \approx X_{n(freeze)} \exp \left[-\left(\frac{0.028 \text{ MeV}}{T} \right)^2 \right]. \quad (9)$$

Combining (6) and (9) and evaluating at T_{freeze} and the BBN temperature T_{BBN} , respectively,

$$X_{n(BBN)} \approx \left[1 + \exp \left[\frac{m_n - m_p}{T_{freeze}} \right] \right]^{-1} \exp \left[-\left(\frac{0.028 \text{ MeV}}{T_{BBN}} \right)^2 \right]. \quad (10)$$

If we can determine T_{freeze} and T_{BBN} then we will know the neutron abundance during BBN. As demonstrated in (5), the proton-to-neutron reaction rate $\lambda(p \rightarrow n)$ falls off more quickly than the neutron-to-proton reaction rate $\lambda(n \rightarrow p)$, and thus the former becomes the limiting case. We define reaction cut off when $\lambda(p \rightarrow n) \sim H$ where H is the rate for the expansion of the universe. For the radiation-dominated era [3, pg 87],

$$H \equiv \frac{\dot{R}}{R} = \left(\frac{8\pi G \rho}{3} \right)^{1/2} = \left(\frac{8\pi^3 G g}{90} \right) T^2, \quad (11)$$

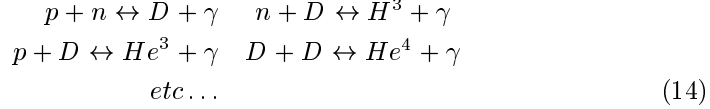
and from (3),

$$\lambda(p \rightarrow n) = \lambda(p + e^- \rightarrow \nu_e + n) + \lambda(p + \bar{\nu}_e \rightarrow e^+ + n) + \lambda(p + e^- + \bar{\nu}_e \rightarrow n). \quad (12)$$

These individual reaction rates have been calculated from the theory of weak interactions [4, 9], and although not difficult, we simply cite the result [3]

$$T_{freeze} \approx 0.8 \text{ MeV}. \quad (13)$$

But what is the BBN temperature T_{BBN} ? The formation of deuterium (D), tritium (H^3), helium-3 (He^3), and helium-4 (He^4) requires an extensive sequence of two-body interactions, i.e.



If we assume that element abundances appear according to thermal equilibrium considerations, then according to Maxwell-Boltzmann statistics (since such nuclei are highly nondegenerate), elements with the highest binding energy appear first, e.g. helium-4 should appear when $T \leq 28.3 MeV$. Indeed, this is not the case since heavier elements must be formed in reactions (see (14)) that involve, most notably, deuterium (except the formation of deuterium itself, which proceeds since it only requires protons and neutrons). Thus, BBN is restrained until temperatures are low enough for deuterium formation.

The binding energy of deuterium is $2.22 MeV$, and so below this temperature we expect BBN to proceed. This also is not the case, however, because the temperature must drop even further to offset the small value of the baryon-to-photon ratio η . This can be seen as follows: the number density of a species with a Fermi (+) or Bose (-) distribution is

$$n = \frac{g}{2\pi^2} \int_0^\infty dp \frac{p^2}{1 \pm \exp\left(\frac{E}{T} - \xi\right)}, \tag{15}$$

where $E = (m^2 + p^2)^{1/2} \approx (m + \frac{p^2}{2m})$. Here we have introduced the dimensionless parameter $\xi = \frac{\mu}{T}$ since the chemical potential μ redshifts as the temperature. We assume the deuterium is nonrelativistic and nondegenerate, so we can use the nonrelativistic Maxwell-Boltzmann approximation

$$n = \frac{g}{2\pi^2} \int_0^\infty dp p^2 \exp\left(\xi - \left(\frac{m + p^2/2m}{T}\right)\right) = g \left(\frac{mT}{2\pi}\right)^{3/2} \exp\left(\xi - \frac{m}{T}\right). \tag{16}$$

Chemical potentials must be conserved in all reactions, so for a nuclide i consisting of Z_i protons and $A_i - Z_i$ neutrons we have $\xi_i = Z_i \xi_p + (A_i - Z_i) \xi_n$, and so

$$\begin{aligned} X_i &= \frac{A_i n_i}{\eta n_\gamma} = g_i \left(\frac{m_i T}{2\pi}\right)^{3/2} \exp\left(Z_i \xi_p + (A_i - Z_i) \xi_n - \frac{m_i}{T}\right) \\ &= g_i \left(\frac{m_i T}{2\pi}\right)^{3/2} \exp(\xi_p)^{Z_i} \exp(\xi_n)^{A_i - Z_i} \exp\left(\frac{m_i}{T}\right), \end{aligned} \tag{17}$$

where η is the baryon-to-photon ratio and n_γ is the photon number density. But

$$X_p \eta n_\gamma \equiv n_p = g_p \left(\frac{m_p T}{2\pi}\right)^{3/2} \exp\left(\xi_p - \frac{m_p}{T}\right)$$

$$= g \left(\frac{mT}{2\pi} \right)^{3/2} \exp(\xi_p) \exp\left(-\frac{m_p}{T}\right), \quad (18)$$

where we observe that $m \equiv m_p \approx m_n$ (except in the exponent) and $g \equiv g_p = g_n$. Rearranging,

$$\exp(\xi_p)^{Z_i} = \left[\frac{X_p \eta n_\gamma \exp\left(\frac{m_p}{T}\right)}{g \left(\frac{mT}{2\pi}\right)^{3/2}} \right]^{Z_i} = X_p^{Z_i} \left[\frac{\eta n_\gamma}{g \left(\frac{mT}{2\pi}\right)^{3/2}} \right]^{Z_i} \exp\left(\frac{m_p}{T}\right)^{Z_i}. \quad (19)$$

Similarly,

$$\exp(\xi_n)^{A_i - Z_i} = X_n^{A_i - Z_i} \left[\frac{\eta n_\gamma}{g \left(\frac{mT}{2\pi}\right)^{3/2}} \right]^{A_i - Z_i} \exp\left(\frac{m_n}{T}\right)^{A_i - Z_i}. \quad (20)$$

combining (17), (19), and (20), and observing that $\frac{m_i}{m} \approx A_i$ we have

$$X_i \approx g_i A_i^{5/2} X_p^{Z_i} X_n^{A_i - Z_i} \epsilon^{A_i - 1} \exp\left(\frac{E_B}{T}\right), \quad (21)$$

where $E_B \equiv Z_i m_p + (A_i - Z_i) m_n - m_i$ is the binding energy and $\epsilon \equiv \eta n_\gamma g^{-1} \frac{mT}{2\pi}^{-3/2}$ is a small number.

It is thus not true that the BBN temperature is $T_{BBN} \sim E_B$, but instead [3, 4]

$$T_{BBN} = \frac{E_B}{(A_i - 1) \log \epsilon} \approx 0.07 \text{ MeV (deuterium)}. \quad (22)$$

Combining (10), (13), and (22) we see that

$$X_{n(BBN)} \approx 0.14. \quad (23)$$

For final element abundances, detailed analysis of a considerable number of rate equations is required. Such has been computed by Peebles [9], and later Wagoner, Fowler, and Hoyle [4]. The result is that almost all of the available neutrons rapidly incorporate themselves into helium-4. More precisely, the overall mass fraction of helium-4 is

$$Y \equiv X_{He^4} \approx 2 X_{n(BBN)} \approx 0.28. \quad (24)$$

Thus, the major constituents of the universe are hydrogen and helium-4.

Note that the production of elements with $A \geq 5$ is highly restrained because of the lack of any stable nuclides with $A = 5$ or $A = 8$, i.e. $\alpha - \alpha$, $p - \alpha$, and $n - \alpha$ nuclides. Furthermore, because of the low value for the baryon-to-photon ratio η , three-body interactions cannot contribute significantly to BBN. Thus, we need only consider elements up to helium-4.

3 Homogeneous neutrino degeneracy

Suppose now we introduce a homogeneous neutrino degeneracy, i.e. each neutrino flavor has a chemical potential ξ_i ($i = e, \mu, \tau$). Here we assume two cases: equal degeneracy for all three neutrino flavors $\xi_e = \xi_\mu = \xi_\tau = \xi$; and electron-neutrino degeneracy alone $\xi_e = \xi$, $\xi_\mu = \xi_\tau = 0$. From now on we will only refer to ξ since the meaning is clear within context. Referring to (15) we see that the number density for massless neutrinos and antineutrinos are

$$n_\nu = \frac{1}{2\pi^2} \int_0^\infty dp \frac{p^2}{1 + \exp\left(\frac{p}{T} - \xi\right)} \quad (25)$$

$$n_{\bar{\nu}} = \frac{1}{2\pi^2} \int_0^\infty dp \frac{p^2}{1 + \exp\left(\frac{p}{T} + \xi\right)}. \quad (26)$$

It is obvious that an electron-neutrino degeneracy ξ affects the rates of the $n \leftrightarrow p$ reactions in Eqs. (3) and (4). If $\xi > 0$ then the excess of neutrinos over antineutrinos favors $n \rightarrow p$ reactions, resulting in a low neutron abundance. Conversely, if $\xi < 0$ then there is a high neutron abundance.

Also, any neutrino degeneracy ξ (positive or negative) increases the energy density of the universe

$$\rho_\nu = \frac{1}{2\pi^2} \int_0^\infty dp \frac{p^3}{1 + \exp\left(\frac{p}{T} - \xi\right)} + \frac{1}{2\pi^2} \int_0^\infty dp \frac{p^3}{1 + \exp\left(\frac{p}{T} + \xi\right)}, \quad (27)$$

which increases the rate of expansion (see Eq. (11)). This affects both the final neutron abundance and BBN itself [10].

The previous calculations performed by Wagoner, Fowler, and Hoyle [4] also apply to the case of homogeneous neutrino degeneracy, and we utilize their methods in the next section to determine homogeneous helium-4, deuterium, and lithium-7 abundances.

4 Inhomogeneous neutrino degeneracy

Consider now an inhomogeneous neutrino degeneracy distribution, such as that discussed by Dolgov and Pagel [11]. There, ξ varies significantly on large scales ($\sim 100 - 1000 Mpc$), thus producing an inhomogeneity in present-day element abundances. Such a model was proposed to reconcile a discrepancy in observed deuterium abundances at high redshift.

Here we are interested in inhomogeneity on a much smaller scale. We do make, however, an immediate observation which simplifies the model considerably. Free-streaming relativistic neutrinos (before decoupling) diffuse away any fluctuations in ξ on scales smaller than the relativistic neutrino horizon. Thus, we can assume that any length scale less than the horizon has a homogeneous neutrino degeneracy.

Our model also assumes that large-scale variations in ξ are negligible so that post-BBN element diffusion eliminates any chemical inhomogeneity before the

present day. Although we have no detailed studies available concerning element diffusion and BBN, it seems reasonable to forbid fluctuations in ξ on scales larger than $\sim 1 Mpc$. By making this assumption, we avoid any CMB constraints that limit models which allow large-scale fluctuations in ξ [11].

With these assumptions, we can propose that BBN occurs in isolated horizon volumes as it does for the case of homogeneous neutrino degeneracy. Since different horizon volumes have different values for ξ , we can characterize the distribution of ξ by a weight distribution $f(\xi)$ which gives the probability that a specific horizon volume has a value of ξ between ξ and $\xi + d\xi$.

Using observed abundances of helium-4, deuterium, and lithium-7, arbitrary forms for $f(\xi)$ have been explored in an effort to expand the allowable bounds for the baryon-to-photon ratio η [12]. Here we consider a more detailed analysis of one physically plausible distribution function $f(\xi)$. Justified by the central limit theorem, we propose $f(\xi)$ takes the form of a Gaussian distribution. By varying the Gaussian width σ_ξ , we can see how the element abundances change with increasing inhomogeneity.

It is important to note that the neutrinos will continue to free-stream up to the present day, but each horizon volume will only maintain thermal equilibrium down to neutrino decoupling temperature $T \sim 2 - 3 MeV$, (here we have neglected neutrino-baryon interactions because of the low density of baryons). Thus, even as early as BBN, the neutrino distribution will be non-thermal as the horizon volumes mix but do not interact. We maintain that such an effect will remain negligible down through BBN, and ignore it completely in our calculations. We also ignore any effect that an inhomogeneous lepton distribution may have on η [8].

5 Effect on big bang nucleosynthesis

We calculated element abundances in the cases of equal degeneracy for all three neutrino flavors ($\xi_e = \xi_\mu = \xi_\tau = \xi$) and electron-neutrino degeneracy alone ($\xi_e = \xi$, $\xi_\mu = \xi_\tau = 0$). These are pictured in the left and right columns, respectively, in Figs. 3 through 5. Considering the nearly identical behavior between these cases, the following discussion applies to both.

In an attempt to generalize our results with respect to variations in η , we explored three cases: $\eta = 1e-10$, $\eta = 4e-10$, and $\eta = 1e-9$. It was established in [12] that for inhomogeneous neutrino degeneracy the acceptable ranges for η are

$$3.0e-10 \leq \eta \leq 1.1e-8 \quad \xi_e = \xi, \quad \xi_\mu = \xi_\tau = 0 \quad (28)$$

$$3.1e-10 \leq \eta \leq 1.0e-9 \quad \xi_e = \xi_\mu = \xi_\tau = \xi \quad (29)$$

We do not, therefore, expect realistic quantities in the case of $\eta = 1e-10$, but here we are only interested in general trends. Also, as discussed in [12], we use a slightly-broadened range for the observed element abundances with which to

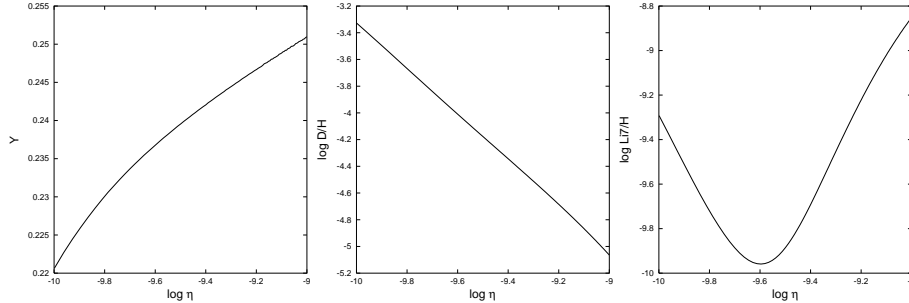


Figure 1: Non-degenerate helium-4, deuterium, and lithium-7 abundances vs. baryon-to-photon ratio η

compare our calculations

$$0.228 \leq Y \leq 0.248 \quad (30)$$

$$-4.7 \leq \log D/H \leq -4.3 \quad (31)$$

$$-10 \leq \log Li7/H \leq -9.4 \quad (32)$$

For each value of η above we calculated five curves (Gaussian mean $\bar{\xi} = -1, -0.5, 0, 0.5, 1$) of the helium-4, deuterium, and lithium-7 abundances versus increasing Gaussian width σ_ξ .

From Fig. 3 we see that in almost all cases the helium-4 abundance increases with increasing Gaussian width σ_ξ . Only for unrealistic helium-4 abundances ($Y > 0.30$) do we observe curves that decrease with increasing inhomogeneity (increasing σ_ξ). We argue that these decreasing curves always remain above the range of interest, and thus can be disregarded. This is readily apparent since the helium-4 abundance in general increases with η (see Fig. 1), and thus only by lowering η further can we bring these curves into the proper range. But $\eta = 1e - 10$ is already below the acceptable range. Accordingly, we disregard the decreasing curves and assert that the helium-4 abundance increases with σ_ξ .

Since the helium-4 abundance increases with η , and as shown it also increases with σ_ξ , we conclude that Gaussian inhomogeneity decreases the upper bound on η , but it also allows for a smaller lower bound.

Similarly, Fig. 4 implies that the deuterium abundance also increases with σ_ξ . Here the effect is ubiquitous. Deuterium abundances, however, decrease with increasing η (see Fig. 1). Therefore, Gaussian inhomogeneity increases the lower bound on η , but it also allows for a larger upper bound.

Combining both the helium-4 and deuterium considerations, we see that Gaussian inhomogeneity increases the lower bound and decreases the upper bound, i.e. the acceptable range for η is narrowed in comparison to homogeneous neutrino degeneracy alone.

The lithium-7 abundances in Fig. 5 also demonstrate this effect. Evidently such abundances increase with Gaussian width σ_ξ , with only a few cases of *meager* exception. But these abundances increase (see Fig. 1) if we vary η in

either direction around some η_0 (where the lithium-7 abundance is a minimum). Thus again the upper bound is decreased and the lower bound is increased.

6 Discussion

Since homogeneous neutrino degeneracy is a special case of inhomogeneous neutrino degeneracy, we expect the latter to yield a widened range of acceptable values for η . Whitmire and Scherrer [12] quantified this result, and found that although inhomogeneous neutrino degeneracy does not significantly decrease the lower bound for η , the upper bound can be increased almost arbitrarily.

For the special case of a Gaussian distribution of inhomogeneous neutrino degeneracy, however, we have shown the opposite effect - the acceptable range of η is narrowed with respect to the homogeneous case. We have only calculated cases where the Gaussian mean $\bar{\xi} \sim 0$, but examination of Fig. 2 and consideration of the observed element abundances reveals that larger degeneracies cannot produce realistic abundances. This is particularly obvious for the deuterium abundance, which is too high when $\xi \ll 0$ and too low when $\xi \gg 0$.

It may be possible, however, to produce Gaussian-like models which do expand the range of η . For example, we could describe inhomogeneity through three different weight distributions $f_i(\xi)$ ($i = e, \mu, \tau$), each giving the probability that a given horizon has a single-flavor neutrino degeneracy between ξ_i and $\xi_i + d\xi_i$. Then the overall element abundance would be

$$\bar{X}_A = \iiint d\xi_e d\xi_\mu d\xi_\tau X_A(\xi_e, \xi_\mu, \xi_\tau). \quad (33)$$

Additionally, variations in ξ_i may result in inhomogeneities in the baryon-to-photon ratio η . Given a functional dependence $\eta = g(\xi_e, \xi_\mu, \xi_\tau)$ we could examine more general models which take this into consideration [8].

7 Acknowledgments

S.D.S. was supported at The Ohio State University by the National Science Foundation Research Experience for Undergraduates (REU) program (NSF PHY-9605064). R.J.S. is supported by the Department of Energy (DE-FG02-91ER40690).

References

- [1] R.A. Malaney and G.J. Mathews, *Phys. Rep.* **229**, 145 (1993)
- [2] S. Weinberg, *Gravitation and Cosmology*, pgs 528-561 (1972)
- [3] T. Padmanabhan, *Structure Formation in the Universe*, pgs 82-122 (1993)
- [4] R.V. Wagoner, W.A. Fowler, and F. Hoyle, *Astrophys. J.* **148**, 3 (1967)
- [5] R.J. Scherrer, *Mon. Not. R. Astron. Soc.* **205**, 683 (1983)
- [6] A. Casas, W.Y. Cheng, and G. Gelmini, *Nucl. Phys.* **B538**, 297 (1999)
- [7] J. McDonald, hep-ph/9908300
- [8] J. March-Russell, H. Murayama, and A. Riotto, *J. High Energy Phys.* **11**, 015 (1999)
- [9] P.J.E. Peebles, *Astrophys. J.* **146**, 542 (1966)
- [10] H.S. Kang and G. Steigman, *Nucl. Phys.* **B372**, 494 (1992)
- [11] A.D. Dolgov and B.E.J. Pagel, *New Astron.* **4**, 223 (1999)
- [12] S.E. Whitmire and R.J. Scherrer, *Phys. Rev. D* **61**, 083508 (2000)

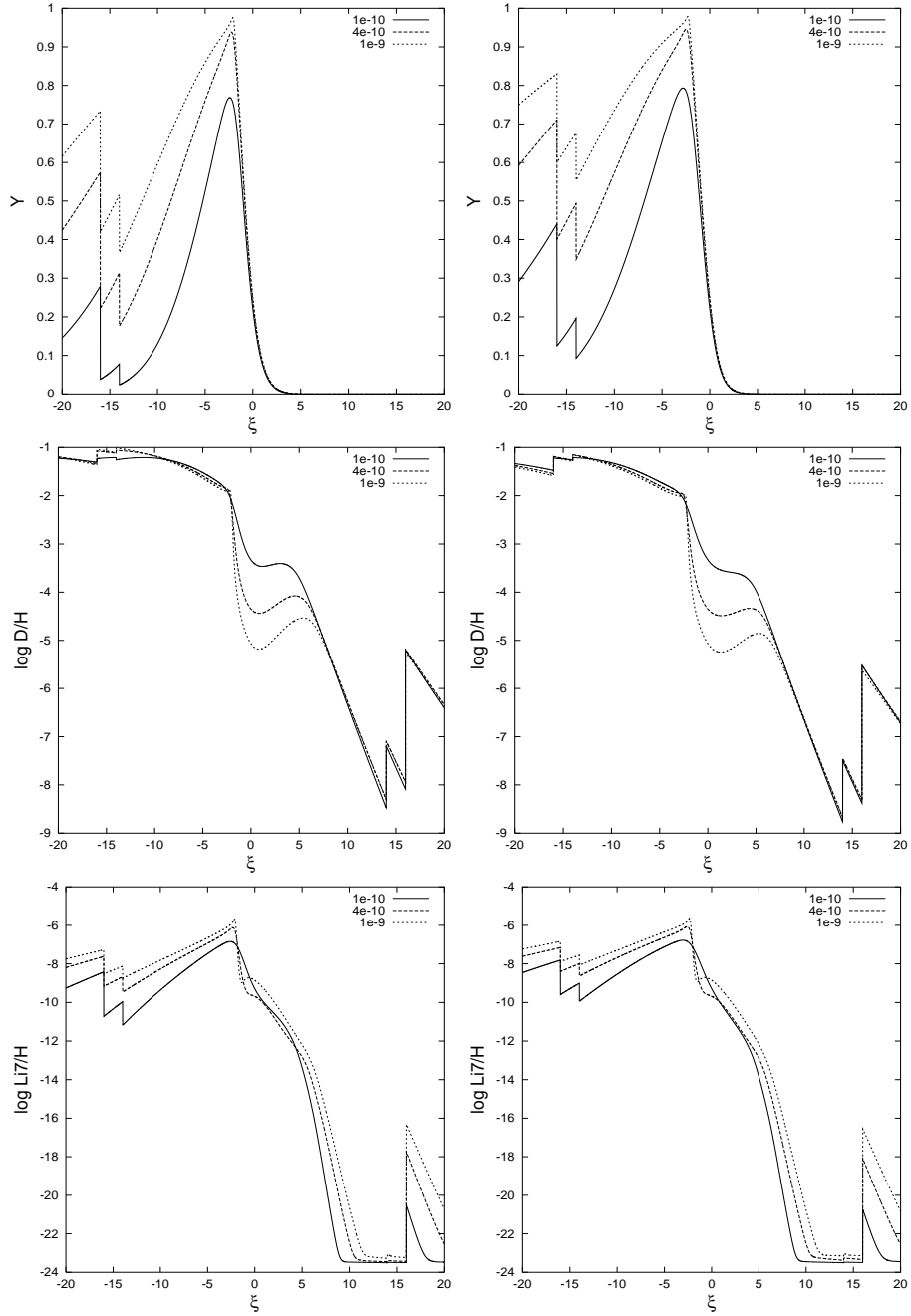


Figure 2: Homogeneous helium-4, deuterium, and lithium-7 abundances vs. neutrino degeneracy ξ
 $\xi_e = \xi = \xi_\mu = \xi_\tau = \xi$ (left) and $\xi_e = \xi$, $\xi_\mu = \xi_\tau = 0$ (right)

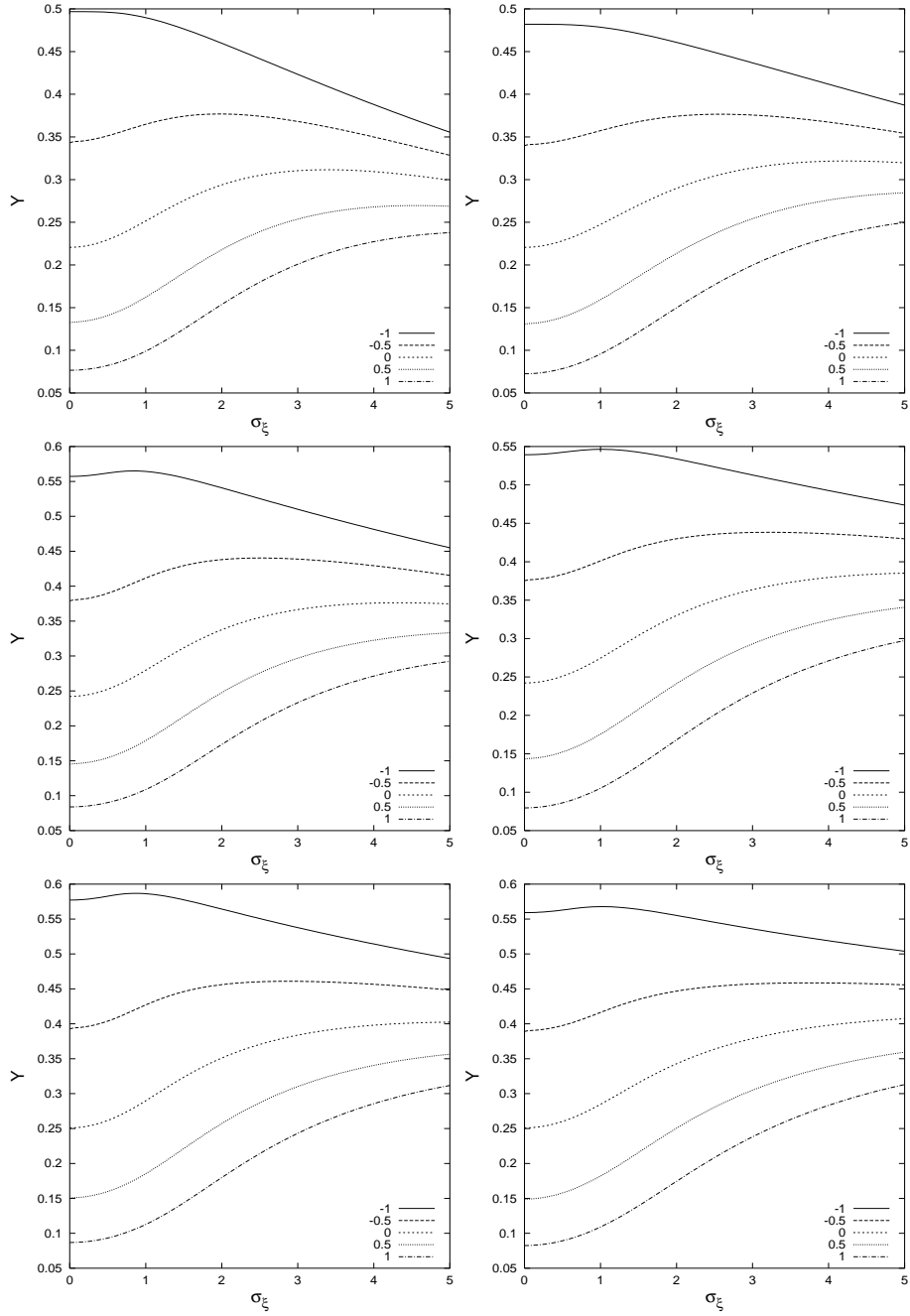


Figure 3: Inhomogeneous helium-4 abundances vs. Gaussian width σ_ξ
 $\xi_e = \xi_\mu = \xi_\tau = \xi$ (left) and $\xi_e = \xi$, $\xi_\mu = \xi_\tau = 0$ (right)
 $\eta = 1e - 10$ (top), $4e - 10$ (center), $1e - 9$ (bottom)

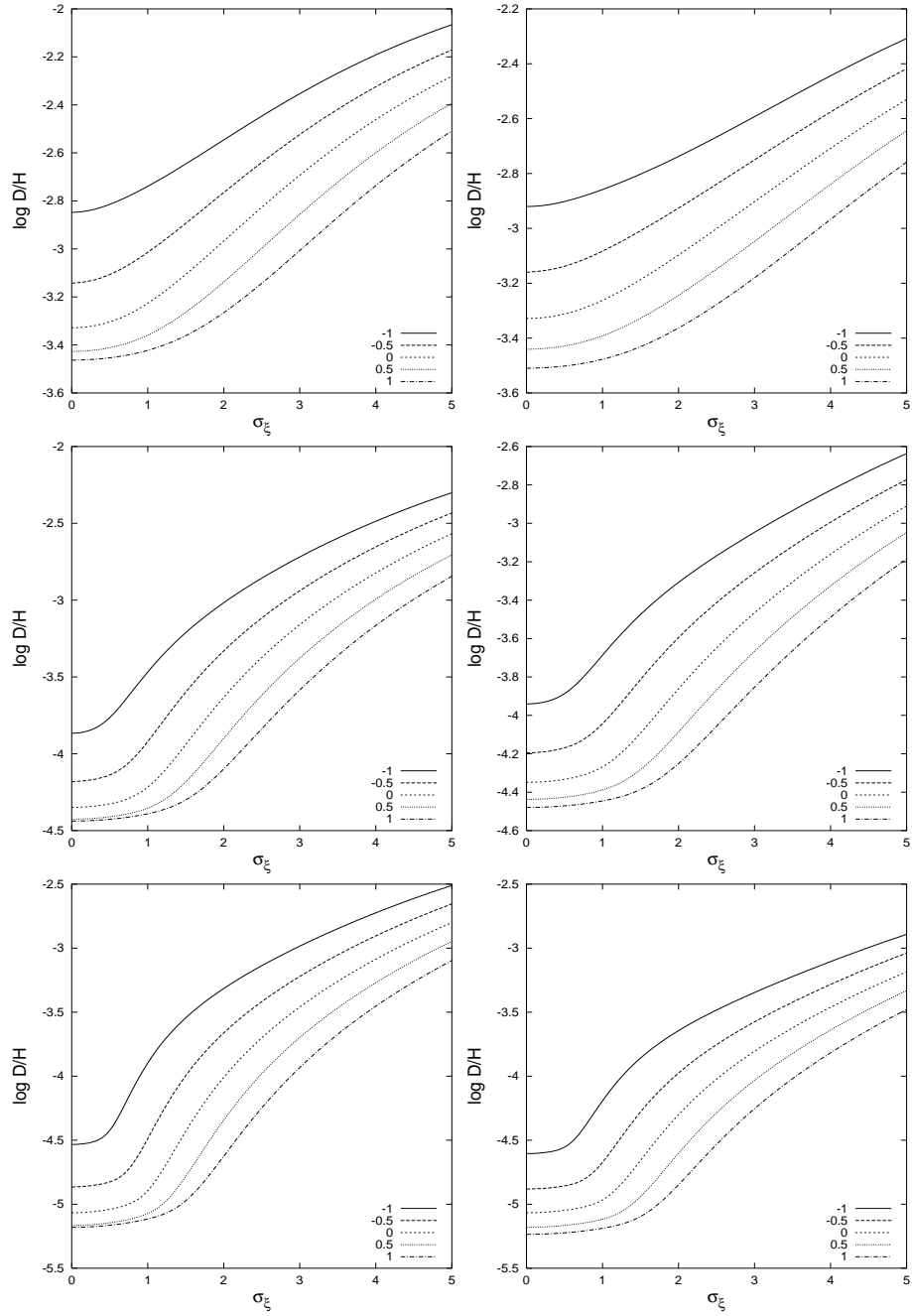


Figure 4: Inhomogeneous deuterium abundances vs. Gaussian width σ_ξ
 $\xi_e = \xi_\mu = \xi_\tau = \xi$ (left) and $\xi_e = \xi$, $\xi_\mu = \xi_\tau = 0$ (right)
 $\eta = 1e-10$ (top), $4e-10$ (center), $1e-9$ (bottom)

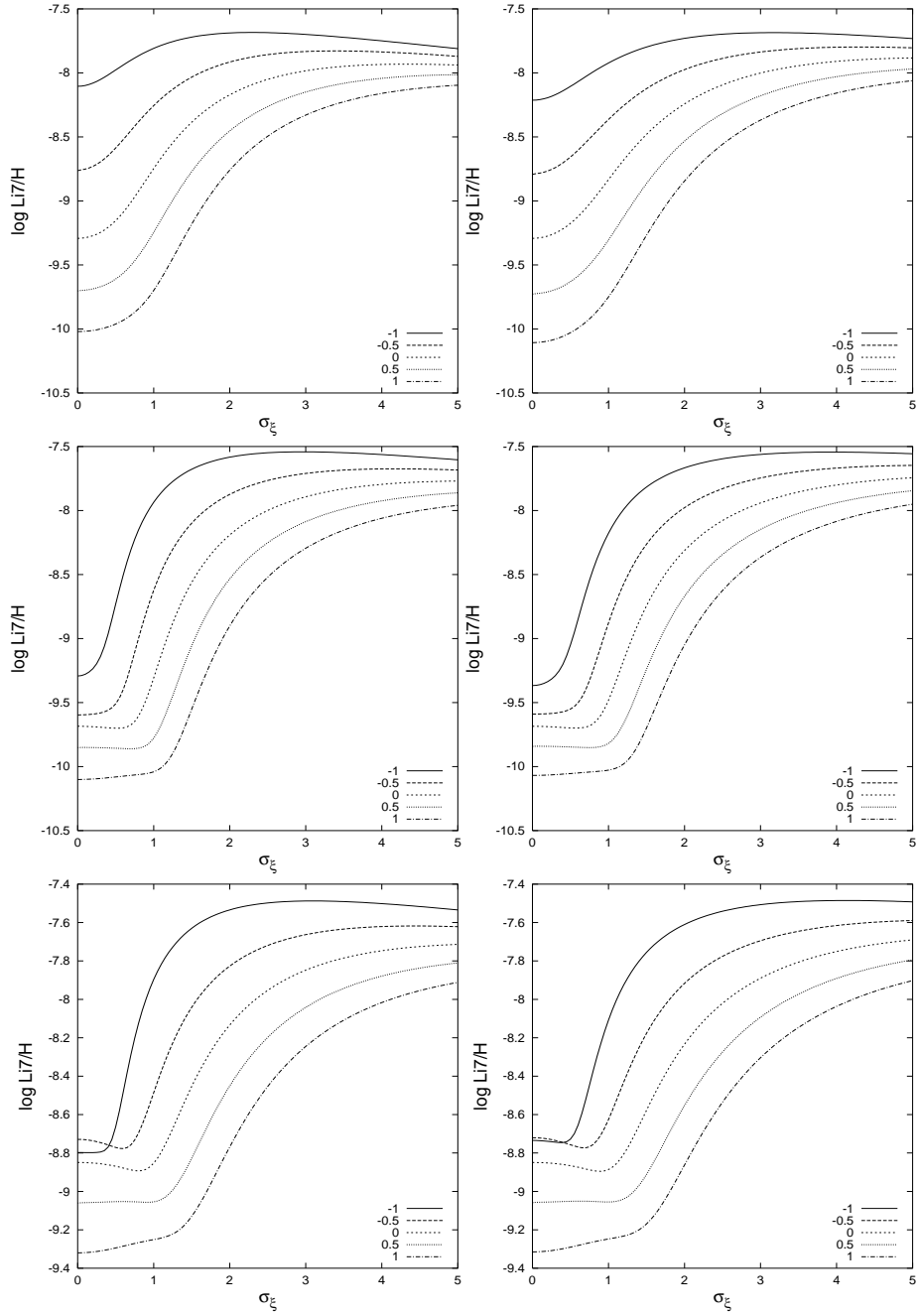


Figure 5: Inhomogeneous lithium-7 abundances vs. Gaussian width σ_ξ
 $\xi_e = \xi_\mu = \xi_\tau = \xi$ (left) and $\xi_e = \xi$, $\xi_\mu = \xi_\tau = 0$ (right)
 $\eta = 1e - 10$ (top), $4e - 10$ (center), $1e - 9$ (bottom)